PNAS
www.pnas.org

1

2 **Main Manuscript for**

3 # Superoxide is promoted by sucrose and affects amplitude of circadian
4 rhythms in the evening

5 Ángela Román[a,b,1,2], Xiang Li[a,1], Dongjing Deng[a,1], John W. Davey[b], Sally James[b], Ian A.
6 Graham[b], Michael J. Haydon[a,b,3]

7 [a]School of BioSciences, The University of Melbourne, Parkville, 3010, Australia

8 [b]Department of Biology, University of York, Wentworth Way, YO10 5DD, United Kingdom

9 [1] These authors contributed equally

10 [2] Current address: Estación Experimental de Aula Dei – CSIC, Zaragoza, E-50059, Spain.

11 [3] Michael J. Haydon
12 **Email:** m.haydon@unimelb.edu.au

13 AR 0000-0003-3457-999X; XL 0000-0002-6325-6439; JWD 0000-0002-1017-9775; IAG 0000-
14 0003-4007-1770; MJH 0000-0003-2486-9387

15 **Classification**

16 Biological Sciences; Plant Biology

17 **Keywords**

18 Circadian, superoxide, sugar, redox, ROS

19 **Author Contributions**

20 MJH conceived the study; AR, XL, DD, MJH designed experiments; AR, XL, DD, JWD, SJ, MJH
21 performed experiments; AR, XL, DD, JWD, IAG, MJH analysed or interpreted data; MJH wrote
22 the manuscript; all authors edited the manuscript.

23 **This PDF file includes:**

24 Main Text
25 Figures 1 to 4

Abstract

Plants must coordinate photosynthetic metabolism with the daily environment and adapt rhythmic physiology and development to match carbon availability. Circadian clocks drive biological rhythms which adjust to environmental cues. Products of photosynthetic metabolism, including sugars and reactive oxygen species (ROS), are closely associated with the plant circadian clock and sugars have been shown to provide metabolic feedback to the circadian oscillator. Here, we report a comprehensive sugar-regulated transcriptome of Arabidopsis and identify genes associated with redox and ROS processes as a prominent feature of the transcriptional response. We show that sucrose increases levels of superoxide (O_2^-) which is required for transcriptional and growth responses to sugar. We identify circadian rhythms of O_2^--regulated transcripts which are phased around dusk and find that O_2^- is required for sucrose to promote expression of *TIMING OF CAB1 (TOC1)* in the evening. Our data reveal a role for O_2^- as a metabolic signal affecting transcriptional control of the circadian oscillator in Arabidopsis.

Significance Statement

Distinguishing the effects of light and sugars in photoautotrophic cells is challenging. The circadian system is a regulatory network that integrates light and metabolic signals and controls rhythmic physiology and growth. Our experimental approach has defined a light-independent, sugar-regulated transcriptome in Arabidopsis and revealed reactive oxygen species (ROS) as a prominent feature. ROS are by-products of photosynthetic metabolism and oscillate with circadian rhythms but have not previously been demonstrated as inputs to the plant circadian oscillator. Our data suggest a new role for superoxide as a rhythmic sugar signal which acts in the evening and affects circadian gene expression and growth.

Main Text

Introduction

Plant metabolism is inextricably linked to daily photoperiodic cycles because of the requirement of light for photosynthesis. Anticipation and adaptation to changing light availability enables plants to optimise metabolism according to their immediate environment. Plant metabolism responds to environmental cues, such as light, temperature, biotic and abiotic stress by diverse mechanisms (1).

Plant cells require signalling mechanisms to sense carbon and energy status and adjust metabolism. Snf1 RELATED KINASE 1 (SnRK1) and TARGET OF RAPAMYCIN 1 (TOR1) are counteracting signalling hubs which are activated under low and replete carbon status, respectively (2, 3). Trehalose-6-phosphate (T6P) is an essential signalling sugar which indicates carbon status and acts through SnRK1 (4, 5).

Circadian clocks are an endogenous time-keeping mechanism which regulate rhythms of physiology and metabolism and control responses to environmental signals according to the time of day (6). The core circadian oscillator in Arabidopsis is a network of transcription factors comprised of Myb-like genes *CIRCADIAN CLOCK ASSOCIATED 1 (CCA1), LATE ELONGATED HYPOCOTYL (LHY)* and *REVIELLE (RVE)* expressed at dawn, *PSEUDO RESPONSE REGULATOR (PRR)* genes expressed through the day including *TIMING OF CAB 1 (TOC1)* at

dusk, and the Evening Complex (EC) in the night. The phase and amplitude of gene expression and protein levels are responsive to environmental cues and they, in turn, coordinate the regulation of thousands of genes.

There is extensive transcriptional and post-transcriptional control of photosynthetic metabolism by the circadian clock and there is metabolic feedback on the circadian oscillator. Elevated SnRK1 activity under carbon limitation lengthens circadian period and sucrose shortens period by T6P-SnRK1 acting on the oscillator gene *PRR7* (7–9). Period also responds to glucose by a TOR-dependent mechanism (10). In continuous dark, circadian rhythms rapidly dampen, but can be sustained by addition of sugars. This effect of sugar requires GIGANTEA (GI), a clock protein which is stabilised by sucrose in the evening (11). Sugars can also reinitiate transcriptional rhythms in dark-adapted seedlings, setting phase according to the time of sugar application (8, 12), but the mechanism in unknown.

Redox state and levels of reactive oxygen species (ROS), which are tightly linked to metabolism, are also associated with circadian rhythms in plants. There are circadian rhythms of hydrogen peroxide (H_2O_2) and $NADP(H)^+$ in Arabidopsis (13, 14). Circadian rhythms of peroxiredoxin oxidation have been detected across Kingdoms (15). These rhythms of redox state and associated ROS are generally considered as outputs of rhythmic metabolism controlled by the circadian clock (13), or even independent of the circadian oscillator (15). The defence hormone salicylic acid perturbs redox state and affects gating of immune response, dependent on the redox-sensitive transcription factor NON-EXPRESSOR OF PATHOGENESIS 1 (NPR1) (14). But there is presently no clear evidence of a role for redox signals as a mechanism of metabolic feedback to the circadian oscillator in plants.

Distinguishing sugar and light signals can be challenging in photosynthetic cells since it is likely that sugar signalling will be activated in the light. Recent advances in our understanding of the impact of metabolic signalling to the plant circadian clock have relied on experiments in low light or darkness (7, 8, 10–12, 16). Here, we use an experimental approach based on the previous observation that sugar can activate expression of circadian clock genes in dark-adapted seedlings to define a light-independent, sugar-regulated transcriptome in Arabidopsis (8, 12). We compare the response of the transcriptome to sucrose in the dark and inhibition of photosynthesis in the light and identify redox and ROS processes as a prominent feature of transcriptional responses to sugars. We demonstrate that superoxide (O_2^-) can act as a signal to alter gene expression and growth in response to sucrose. This O_2^- signal acts to promote transcription of circadian oscillator genes in the evening. These reveal that ROS can function as metabolic signals affecting circadian rhythms in Arabidopsis.

Results

To identify transcripts that are regulated by sugars in the presence and absence of light and photosynthesis, we designed an RNA-seq experiment based on the previous observation that sugars can reinitiate transcriptional circadian rhythms in dark-adapted Arabidopsis seedings (8, 12). Two-week old wild-type (Col-0) seedings were grown in the dark for 72 h to dampen circadian rhythms and establish a stabilised C starvation state. At subjective dawn, dark-adapted seedlings were transferred to media containing 10 mM mannitol (osmotic control) or sucrose and maintained in the dark or transferred to media containing 10 mM mannitol with or without 3-(3,4-dichlorophenyl)-1,1-dimethylurea (DCMU), an inhibitor of photosynthesis, and grown in the light. The four treatments provide conditions of no sugar/no light (Dark), sugar/no light (Suc), sugar/light (Light) and light/no sugar (DCMU) (Fig. 1A). We confirmed that seedling glucose content increased in the Suc and Light treatments but not in the Dark or DCMU treatments (Fig. 1B). To capture both early and late transcriptional responses within the timeframe of a typical photoperiod, shoot tissue was harvested at subjective dawn (0 h) and 0.5, 2 and 8 h after the treatments and prepared for RNA-Seq.

We detected 5571 Suc-regulated genes that were differentially expressed between Dark and Suc treatments and 4628 DCMU-regulated genes differentially expressed between Light and DCMU (Fig. 1C, Dataset 1). The quantification of gene expression by RNA-seq was corroborated for 31 representative transcripts by qRT-PCR with a strong positive correlation (R^2=0.91) (Fig. S1). The overlap of differentially expressed genes (DEGs) between time-points was relatively low (Fig. 1C), suggesting the sampling design captures a wide dynamic range of the transcriptional response. Comparison of our list of Suc-regulated genes to published microarray datasets (17, 18) indicated that we have captured a more extensive sugar-regulated transcriptome (Fig. S2A).

To identify genes that are regulated by sugar, independent of light availability, we generated a list of genes that were upregulated by Suc in the dark and downregulated by DCMU in the light (sugar-activated; 927) or downregulated by Suc in the dark and upregulated by DCMU in the light (sugar-repressed; 1117) (Dataset 2; Fig. S3). The sugar-activated genes were enriched for Gene Ontology (GO) terms related to protein and cell wall synthesis (Fig. S3A). Sugar-repressed genes were enriched for GO terms related to light signalling, circadian rhythm and sugar metabolism (Fig. S3B, S3C). We compared our list of all 2042 sugar-regulated genes to published lists of genes regulated by SnRK1 and TOR, which are two major energy signalling hubs (2, 3). There was significant overlap with both datasets, but 1080 sugar-regulated genes were unique to this study (Fig. S3D), including 929 genes represented on ATH1 microarrays. These unique genes could represent responses either upstream or independent of SnRK1- and TOR-mediated signalling. Among the most significantly enriched GO terms in this list was Response to oxygen containing compound and Circadian rhythm (Fig. S3E).

To define the temporal characteristics of the complete transcriptome dataset, we performed clustering analysis of expression of 18071 genes across all 53 samples using variational Bayesian Gaussian mixture models (Fig. 1D, Dataset 3). We opted for 14 clusters as a tradeoff between maximizing the explained variance and producing meaningful clusters (Fig. S4, Fig. 1D). Several clusters were associated with either sugar-repressed (clusters 1-4) or sugar-activated (clusters 11-14) genes (Fig. 1D). We searched for enriched GO terms within each cluster (Dataset 3) and summarised these using an enrichment map of the top 15 terms within each cluster (Fig. 1E, Dataset 4). Some highly enriched GO term networks were specific to one or two clusters such as inositol phosphate processes in cluster 13 or circadian rhythm and growth in clusters 8 and 13. Other enrichment GO term networks represent four or five clusters. The largest of these networks included terms associated with metabolism of sugars, nucleotides and phospholipids, chloroplast function and proteostasis. The second largest enrichment network included terms associated with reactive oxygen species (ROS) metabolism and signalling, metabolic stress and immune responses.

Since GO terms associated with ROS appear to be a strong feature of the complete dataset, we hypothesised that ROS might be contributing to transcriptional responses to sugar. Indeed, Response to oxygen containing compound was the most significantly enriched GO term among all 2042 sugar-regulated genes and among Suc-regulated genes at 2 h (Fig. S2B). Within the former, 195 genes are associated with this GO term, including *ANNEXIN 2 (ANN2)* and six *WRKY* transcription factor genes (Fig. 2A, Dataset 5). We also identified 95 sugar-regulated genes previously reported as ROS-responsive (19), including *ASCORBATE PEROXIDASE 1 (APX1)* and *CATALASE 2 (CAT2)* (Fig. 2B, Dataset 5).

To test whether treatment of Arabidopsis seedlings with sucrose affects production of ROS in dark-adapted seedlings, we used histochemical stains for hydrogen peroxide (H_2O_2) and superoxide (O_2^-) (Fig. 2C,D). Treatment of dark-adapted seedlings with sucrose led to a decrease in staining for H_2O_2 within 30 min. By contrast, sucrose treatment of dark-adapted seedlings increased stain for O_2^- within 2 h, compared to mannitol controls. The elevated NBT stain was observed throughout the shoot, including hypocotyl, cotyledons and leaves. To corroborate this

observation, we used a L-012 luminescence assay, which does not discriminate between H_2O_2 and O_2^-, but provides better temporal resolution of ROS production than histochemical stains. Consistent with the NBT stains for O_2^-, we detected elevated L-012 luminescence within 2 h in sucrose-treated seedlings compared to mannitol-treated controls (Fig. 2E). Presumably, this assay underestimates the difference in O_2^- production since the signal in sucrose-treated seedlings will be the sum of the reduced H_2O_2 and the increased O_2^- (Fig. 2C). The ROS-response detected in both the histochemical and luminescent assays is concomitant with the timing of the transcriptional response associated with ROS-related genes that we detected after 2 h (Fig. 2A, 2B, S2B, Dataset 1).

The accumulation of O_2^- in sucrose-treated seedlings might be a by-product of increased energy metabolism or could be contributing as a signal to affect transcriptional changes. We looked for chemicals that could inhibit the sucrose-induced production of O_2^-. Diphenyleneiodonium (DPI) is an inhibitor of NADPH oxidases, which generate O_2^- at the plasma membrane. Methyl viologen (MV) interferes with electron transport from PS I and elevates O_2^-. 3-amino-1,2,4-triazole (3-AT) is a catalase inhibitor which promotes H_2O_2 accumulation. We tested the effect of these chemicals on induction of a circadian-regulated luciferase reporter for *COLD, CIRCADIAN RHYTHM REGULATED 2 (CCR2)*. DPI strongly inhibited the increase of luciferase luminescence in sucrose-treated, dark-adapted *CCR2p:LUC* seedlings, whereas MV and 3-AT did not (Fig. 3A). Similarly, DPI, but not MV or 3-AT, also inhibited sucrose-induced L-012 luminescence (Fig. 3B) and histochemical staining for O_2^- but did not affect sucrose-induced changes in staining for H_2O_2 (Fig. 3C, D).

We used the transcriptional response of *CCR2p:LUC* to generate a dose-response curve of inhibition by DPI. This response was inhibited by 30% at 1 µM DPI and by >70% at concentrations above 5 µM (Fig. 3E). Similar dose-dependent effects were also observed for two other NADPH oxidsase inhibitors, VAS2870 (20) and apocynin (21), but not for the xanthine dehydrogenase inhibitor, allopurinol (22) (Fig S5). We confirmed that DPI also inhibited sucrose-induction of *CCR2* and *WRKY60* transcripts by qRT-PCR (Fig. 3F) as well as *WRKY11p:ß-GLUCURONIDASE (GUS)* and *WRKY30p:GUS* reporters (Fig. S6). Thus, DPI effectively inhibits transcriptional regulation of multiple sugar-regulated genes.

DPI could be inhibiting transcriptional responses to sugar in our assay by affecting uptake of sucrose, altered sugar metabolism, or inhibition of sugar sensing or signalling. We measured soluble sugars glucose, fructose and sucrose in sucrose-treated dark-adapted seedlings in the presence of DMSO or DPI. We did not detect a difference from controls for any sugar within 8 h of sucrose treatment (Fig. S7), suggesting that inhibition of sugar uptake or sucrose catabolism cannot account for the dramatic inhibition of the transcriptional response by DPI.

Since DPI can inhibit transcriptional responses to sugar, we sought to establish whether DPI also affects other sugar-regulated processes in Arabidopsis. Seed germination in both dormant and non-dormant seeds is inhibited by exogenous sugar, acting through abscisic acid-dependent pathways (23). Similarly to sucrose, DPI also inhibits germination (24) (Fig. S8). If DPI inhibits germination by the same pathway as sucrose, we expected that their effects would be non-additive. However, the effect of DPI on inhibition of germination was detected both with and without sucrose in dormant and non-dormant seeds (Fig. S8). This suggests that DPI does not affect the regulatory pathways through which sucrose inhibits seed germination.

Sugars promote growth. To test the effect of DPI on growth promotion by sucrose, we measured effects on hypocotyl elongation and root growth in dark-grown seedlings. This growth assay enables quantification of effects of sugar on cell elongation in the hypocotyl and cell division in the root in the absence of light signals. Seedlings growing on media containing DPI had slightly reduced hypocotyl length and root length in control media, and DPI strongly attenuated the

positive effects of sucrose on both hypocotyl and root length (Fig 3G). These data suggest that DPI inhibits the signalling or metabolism of sucrose to promote cell elongation and cell division.

NADPH oxidases are encoded by a family of ten *RESPIRATORY BURST OXIDASE HOMOLOG (RBOH)* genes in Arabidopsis. We tested whether *rboh* mutants had altered ROS production in dark-adapted seedlings using L-012 luminescence assays. Both the *rbohb* and *rbohc* mutants had similar response to sucrose as wild type, but *rboha* mutants and *rbohd rbohf* double mutants had reduced L-012 luminescence (Fig. S9A), similar to wild type treated with DPI, VAS2890 or apocynin (Fig. S5B). We also tested whether *rboh* mutants had altered growth responses to sucrose (Fig. S9B). The *rbohd rbohf* double mutant had reduced root and hypocotyl length on control media compared to wild type but growth was still responsive to sucrose in the mutant. Stimulation of hypocotyl growth by sucrose was reduced in the *rboha* mutant compared to wild type, but stimulation of root growth was unaffected. Thus, although we detected small growth effects in the mutants, none of those tested were able to phenocopy the effect of DPI. Similarly, the transcriptional response of *CCR2* or *WRKY60* to sucrose in dark adapted seedlings was not reduced in *rboh* mutants (Fig. S9C). These suggest that there is residual O_2^- accumulation in these mutants sufficient to elicit a response and that there is genetic redundancy in the molecular targets of DPI contributing to these sugar responses.

Sugars affect period of circadian rhythms (8) and the circadian clock contributes to rhythms of ROS homeostasis (13). We tested the effect of DPI, MV and 3-AT on circadian rhythms in media with or without sucrose. We measured circadian rhythms of *TOC1p:LUC* in continuous low light (10 µmol m^{-2} s^{-1}) because the effect of exogenous sucrose on circadian rhythms is more pronounced in these conditions (8). Circadian period was significantly shorter in seedlings grown on sucrose compared to mannitol for all ROS modifiers, similar to the DMSO control (Fig. 4A, 4B). This suggests that these chemicals did not affect the adjustment of period by exogenous sucrose.

Sugars also affect amplitude of circadian rhythms (11). Luciferase signal is dramatically elevated in *TOC1p:LUC* seedlings transferred to media containing sucrose compared to mannitol (Fig 4A, 4C). This transcriptional response does not require GI (Fig. S10), a clock protein which is post-transcriptionally regulated by sucrose (11). The effect of sucrose in *TOC1p:LUC* seedlings was strongly attenuated in the presence of DPI, elevated in the presence of MV and unaffected by 3-AT (Fig. 4C), which is consistent with the effects of these compounds on O_2^- levels. The effects of DPI and MV were particularly pronounced during the night and were not observed in *CCA1p:LUC* or *PRR7p:LUC* seedlings (Fig. 4C), suggesting O_2^- acts on specific components of the oscillator.

Since the effects of DPI and MV differed between the morning-phased CCA1p:LUC and PRR7p:LUC and evening-phased TOC1p:LUC, we wondered whether this might reflect a global pattern of O_2^- on transcriptional rhythms. We used a set of previously reported O_2^-- and H_2O_2-responsive transcripts (19) to determine their phases in continuous light from a published RNA-seq dataset (25). The distribution of phases of transcripts up- and down-regulated by O_2^- or H_2O_2 deviated significantly from expectations (Fig. 4D, Dataset 5). The phase of transcripts upregulated by H_2O_2 were enriched several hours after subjective dawn and downregulated transcripts were enriched before subjective dawn. This is consistent with the reported role of CCA1 in driving rhythms of H_2O_2 which peak in the early morning (13). By contrast, the phase of transcripts upregulated by O_2^-, which included *TOC1, GI, PRR5* and *LUX*, were enriched around subjective dusk. About 20% of these genes are direct *TOC1* targets (26) (Dataset 5). Transcripts down-regulated by O_2^-, including *LHY* and *RVE8,* were enriched around subjective dawn. This suggests that H_2O_2 and O_2^- production or signalling are antiphased and is consistent with a role of O_2^- contributing to promoting oscillations of circadian transcripts in the evening.

Discussion

We have identified ROS-regulated genes as a prominent feature in the response of the Arabidopsis transcriptome to sugars in both dark and light (Fig.1). The transcriptional response to sucrose in dark-adapted seedlings coincides with an increase in ROS levels, including O_2^- (Fig. 2). Both the accumulation of O_2^- and transcriptional response to sucrose were strongly attenuated in seedlings treated with DPI, a chemical inhibitor of flavoenzymes including NADPH oxidases (Fig. 3). DPI also inhibited the promotion of hypocotyl elongation and root growth by sucrose, demonstrating a broader impact of the ROS signal in sugar responses. Finally, we found that DPI inhibited the effect of sucrose on the evening expressed *TOC1* and identified a highly significant anti-phasing of rhythmic transcripts that are up- and down-regulated by O_2^- to dusk and dawn, respectively (Fig. 4). This is different to the redox effects of salicylic acid on both morning and evening genes (14). Thus, we propose that O_2^- functions as a metabolic signal associated with sugar levels which acts positively on the circadian oscillator in the evening. An association between cellular sugar status and redox state has been long recognised in the context of metabolism and oxidative stress (27), but our data provide evidence of a role for O_2^- as a dynamic sugar signal affecting daily rhythms of gene expression. This effect of sugar on the oscillator appears to be distinct from the T6P/SnRK1-mediated effect on period *via* transcriptional regulation of *PRR7* (7) (Fig. 4) and the post-transcriptional control of GI (11) (Fig. S9) revealing an additional layer of metabolic control of circadian rhythms in plants.

DPI is a potent inhibitor of NADPH oxidases which generate extracellular O_2^- at the plasma membrane activated by intracellular signals (28). We observed reduced sucrose-activated ROS production and modest growth phenotypes in *rboha* and *rbohd rbohf* mutants, but the transcriptional response to sucrose was similar to wild type (Fig. S8). Notwithstanding that the five *rboh* mutants examined here represent over 90% of total *RBOH* gene expression (Dataset 1), the subtle phenotypes in the *rboh* mutants compared to DPI-treated seedlings probably reflects functional redundancy within this gene family. This will be challenging to verify, since higher order mutants would be expected to be lethal. It is possible that effects of DPI on O_2^--mediated responses to sugar can be attributed to inhibition of other flavoenzymes. For example, in photosynthetic organisms DPI inhibits O_2^- production from xanthine dehydrogenases, glutathione reductases and mitochondrial NAD(P)H dehydrogenases (29–31). However, the similar effects of VAS2890 and apocynin, but not allopurinol, on sugar responses support the role of NADPH oxidases (Fig. S5).

MV interferes with electron transport from PSI, as well as in mitochondria (32), and leads to accumulation of O_2^-, so the opposite effects on transcriptional responses might be expected compared to DPI. MV was unable to induce a transcriptional response in *CCR2p:LUC* seedlings without sucrose (Fig. 3A), which suggests that O_2^- alone does not activate circadian gene expression or that the site of O_2^- accumulation in MV-treated seedlings is not sufficient to act as the signal. However, MV elevated the response to sucrose in *TOC1p:LUC* seedlings (Fig. 4C) suggesting that O_2^- and sucrose might act synergistically.

O_2^- is generated in mitochondria, chloroplasts, peroxisomes and the apoplast (28). O_2^- is typically scavenged quickly by superoxide dismutases. Elevation of O_2^- could be due to increased production or reduced scavenging. The increase in O_2^- triggered by sucrose in dark-adapted seedlings by histochemical stain and L-012 assay was relatively low and slow compared to elicitor-induced respiratory burst (33) but faster than a ROS effect reported for cell-wall damage (34). It might be that sucrose generates O_2^- in specific cell-types or subcellular locations and the signal might be diluted in bulk tissues or our detection methods might have insufficient sensitivity. This might explain why we couldn't detect L-012 luminescence in *rbohd rbohf* double mutants (Fig S8A). Thus, it will be useful to map the cellular and subcellular location of the O_2^- signal using the

expanding toolset of available redox probes (35–37). This will also provide clearer identity of candidate proteins producing the signal.

Reversible oxidation of redox-sensitive proteins by ROS can alter their activity. In Arabidopsis, redox-sensitive proteins that are oxidised by H_2O_2 have been identified in most cellular compartments (38). These include plasma membrane receptors (39), glycolytic enzymes (38, 40) which can localise in the nucleus and associate with DNA (41, 42) and transcription factors (43). Thus, localised changes in redox state could affect signalling pathways and gene expression by various mechanisms. Changes in localised O_2^- concentration could modify protein function indirectly after dismutation to H_2O_2, or directly by affecting Fe-S proteins (28).

It is experimentally difficult to separate the effects of H_2O_2, O_2^- or other ROS on protein oxidation. Differences in target specificity for ROS might depend on their redox dynamics or subcellular location. H_2O_2 is regarded as the most likely ROS signal because it is relatively stable compared to the more reactive O_2^- (28). However, our phase analyses of H_2O_2 and O_2^- regulated transcripts indicates clear temporal separation of their effects (Fig. 4). This might reflect differences in spatial organisation of oxidative metabolism at different times of day. The mechanism by which sugar-activated O_2^- production affects gene regulation will depend on its cellular location.

By examining the effects of sugar on the Arabidopsis transcriptome independently of light, we have uncovered a role for redox status, exemplified by accumulation of O_2^-, that promotes responses to sugar including growth and circadian rhythms. In contrast to the previously reported association of circadian rhythms of H_2O_2, which are phased in the morning (13), the O_2^--activated transcriptome peaks in the evening and includes core genes within the circadian oscillator. Sugar promotes O_2^- which alters gene expression by either an extracellular or intracellular redox signal which could transmit to the nucleus via signalling or protein localisation. We propose that this metabolic signal functions to coordinate rhythmic physiology and growth in response to environmental conditions that affect photosynthetic metabolism.

Materials and Methods

Details of plant materials and growth conditions, RNA-Seq and clustering, qRT-PCR, histochemical stains, luminescence assays and sugar quantification are described in SI Appendix. Primers are listed in Dataset 6.

Acknowledgments

We thank Ms. Heather Eastmond (University of York) for technical support and Prof Alex Webb (University of Cambridge) for useful comments on the manuscript. This research was funded by BBSRC grant (BB/L021188/1) to MJH and IAG, Royal Society Research Grant (RG150144) to MJH and by The University of Melbourne through the Research Grants Support Scheme to MJH and a Melbourne Research Scholarship to XL. This research was not funded by the Australian Research Council.

References

1. H. A. Herrmann, J. M. Schwartz, G. N. Johnson, Metabolic acclimation - A key to enhancing photosynthesis in changing environments? *J. Exp. Bot.* **70**, 3043–3056 (2019).

2. E. Baena-González, F. Rolland, J. M. Thevelein, J. Sheen, A central integrator of transcription networks in plant stress and energy signalling. *Nature* **448**, 938–42 (2007).

3. Y. Xiong, *et al.*, Glucose-TOR signalling reprograms the transcriptome and activates meristems. *Nature* **496**, 181–6 (2013).

4. H. Schluepmann, T. Pellny, A. van Dijken, S. Smeekens, M. Paul, Trehalose 6-phosphate is indispensable for carbohydrate utilization and growth in Arabidopsis thaliana. *Proc. Natl. Acad. Sci. U. S. A.* **100**, 6849–6854 (2003).

5. C. Nunes, *et al.*, The Trehalose-6-phosphate / SnRK1 signaling pathway primes growth recovery following relief of sink limitation. *Plant Phsyiology* **162**, 1720–1732 (2013).

6. M. J. Haydon, X. Li, M. K. Y. Ting, Temporal control of plant-environment interactions by the circadian clock. *Annu. Plant Rev. online* **2**, 1–32 (2019).

7. A. Frank, *et al.*, Circadian Entrainment in Arabidopsis by the Sugar-Responsive Transcription Factor bZIP63. *Curr. Biol.* **28**, 2597-2606.e6 (2018).

8. M. J. Haydon, O. Mielzcarek, F. C. Robertson, K. E. Hubbard, A. a. R. Webb, Photosynthetic entrainment of the Arabidopsis circadian clock. *Nature* **502**, 689–692 (2013).

9. J. Shin, *et al.*, The metabolic sensor AKIN10 modulates the Arabidopsis circadian clock in a light-dependent manner. *Plant Cell Environ.* **40**, 997–1008 (2017).

10. N. Zhang, *et al.*, Metabolite-mediated TOR signaling regulates the circadian clock in Arabidopsis. *Proc. Natl. Acad. Sci. U. S. A.* **116**, 25395–25397 (2019).

11. M. J. Haydon, O. Mielczarek, A. Frank, Á. Román, A. A. R. Webb, Sucrose and ethylene signaling interact to modulate the circadian clock. *Plant Physiol.* **175**, pp.00592.2017 (2017).

12. N. Dalchau, *et al.*, The circadian oscillator gene GIGANTEA mediates a long-term response of the Arabidopsis thaliana circadian clock to sucrose. *Proc. Natl. Acad. Sci. U. S. A.* **108**, 5104–5109 (2011).

13. A. G. Lai, *et al.*, CIRCADIAN CLOCK-ASSOCIATED 1 regulates ROS homeostasis and oxidative stress responses. *Proc. Natl. Acad. Sci.* **109**, 17129–17134 (2012).

14. M. Zhou, *et al.*, Redox rhythm reinforces the circadian clock to gate immune response. *Nature* **523**, 472–476 (2015).

15. R. Edgar, *et al.*, Peroxiredoxins are conserved markers of circadian rhythms. *Nature* **485**, 459–464 (2012).

16. E. Shor, I. Paik, S. Kangisser, R. Green, E. Huq, PHYTOCHROME INTERACTING FACTORS mediate metabolic control of the circadian system in Arabidopsis. *New Phytol.* **215**, 217–228 (2017).

17. K. E. Thum, M. J. Shin, P. M. Palenchar, A. Kouranov, G. M. Coruzzi, Genome-wide investigation of light and carbon signaling interactions in Arabidopsis. *Genome Biol.* **5**, R10 (2004).

18. D. Osuna, *et al.*, Temporal responses of transcripts , enzyme activities and metabolites after adding sucrose to carbon-deprived Arabidopsis seedlings. *Plant J.* **49**, 463–491 (2007).

19. I. Gadjev, *et al.*, Transcriptomic footprints disclose specificity of reactive oxygen species signaling in Arabidopsis. *Plant Physiol.* **141**, 436–445 (2006).

20. S. Mangano, *et al.*, Molecular link between auxin and ROS-mediated polar growth. *Proc.*

436 *Natl. Acad. Sci. U. S. A.* **114**, 5289–5294 (2017).

437 21. J. Stolk, T. J. Hiltermann, J. H. Dijkman, A. J. Verhoeven, Characteristics of the inhibition
438 of NADPH oxidase activation in neutrophils by apocynin, a methoxy-substituted catechol.
439 *Am. J. Respir. Cell Mol. Biol.* **11**, 95–102 (1994).

440 22. C. Hesberg, R. Hänsch, R. R. Mendel, F. Bittner, Tandem orientation of duplicated
441 xanthine dehydrogenase genes from Arabidopsis thaliana: Differential gene expression
442 and enzyme activities. *J. Biol. Chem.* **279**, 13547–13554 (2004).

443 23. J. Price, T. C. Li, S. G. Kang, J. K. Na, J. C. Jang, Mechanisms of glucose signaling
444 during germination of Arabidopsis. *Plant Physiol.* **132**, 1424–1438 (2003).

445 24. K. Müller, A. C. Carstens, A. Linkies, M. A. Torres, G. Leubner-metzger, The NADPH-
446 oxidase AtrbohB plays a role in Arabidopsis seed after-ripening. *New Phytol.* **184**, 885–
447 897 (2009).

448 25. A. Romanowski, R. G. Schlaen, S. Perez-Santangelo, E. Mancini, M. J. Yanovsky, Global
449 transcriptome analysis reveals circadian control of splicing events in Arabidopsis thaliana.
450 *Plant J.* **103**, 889–902 (2020).

451 26. W. Huang, *et al.*, Mapping the core of the Arabidopsis circadian clock defines the network
452 structure of the oscillator. *Science (80-.).* **336**, 75–79 (2012).

453 27. I. Couée, C. Sulmon, G. Gouesbet, A. El Amrani, Involvement of soluble sugars in reactive
454 oxygen species balance and responses to oxidative stress in plants. *J. Exp. Bot.* **57**, 449–
455 459 (2006).

456 28. N. Smirnoff, D. Arnaud, Hydrogen peroxide metabolism and functions in plants. *New*
457 *Phytol.* **221**, 1197–1214 (2019).

458 29. M. Zarepour, *et al.*, Xanthine dehydrogenase AtXDH1 from Arabidopsis thaliana is a
459 potent producer of superoxide anions via its NADH oxidase activity. *Plant Mol. Biol.* **72**,
460 301–310 (2010).

461 30. J. M. Diaz, *et al.*, NADPH-dependent extracellular superoxide production is vital to
462 photophysiology in the marine diatom Thalassiosira oceanica. *Proc. Natl. Acad. Sci. U. S.*
463 *A.* **116**, 16448–16453 (2019).

464 31. T. H. Roberts, K. M. Fredlund, I. M. Møller, Direct evidence for the presence of two
465 external NAD(P)H dehydrogenases coupled to the electron transport chain in plant
466 mitochondria. *FEBS Lett.* **373**, 307–309 (1995).

467 32. F. Cui, *et al.*, Interaction of methyl viologen-induced chloroplast and mitochondrial
468 signalling in Arabidopsis. *Free Radic. Biol. Med.* **134**, 555–566 (2019).

469 33. J. M. Smith, A. Heese, Rapid bioassay to measure early reactive oxygen species
470 production in Arabidopsis leave tissue in response to living Pseudomonas syringae. *Plan*
471 *Methods* **10**, 6 (2014).

472 34. L. Denness, *et al.*, Cell Wall Damage-Induced Lignin Biosynthesis Is Regulated by a
473 Reactive Oxygen Species- and Jasmonic Acid-dependent Process in Arabidopsis. *Plant*
474 *Physiol.* **156**, 1364–1374 (2011).

475 35. A. J. Meyer, *et al.*, Redox-sensitive GFP in Arabidopsis thaliana is a quantitative biosensor
476 for the redox potential of the cellular glutathione redox buffer. *Plant J.* **52**, 973–986 (2007).

36. T. Nietzel, *et al*., The fluorescent protein sensor roGFP2-Orp1 monitors in vivo H 2 O 2 and thiol redox integration and elucidates intracellular H 2 O 2 dynamics during elicitor-induced oxidative burst in Arabidopsis. *New Phytol.* **221**, 1649–1664 (2019).

37. J. Steinbeck, *et al*., In vivo NADH/NAD+ biosensing reveals the dynamics of cytosolic redox metabolism in plants. *Plant Cell* **32**, 3324–3345 (2020).

38. P. Liu, H. Zhang, H. Wang, Y. Xia, Identification of redox-sensitive cysteines in the arabidopsis proteome using OxiTRAQ, a quantitative redox proteomics method. *Proteomics* **14**, 750–762 (2014).

39. F. Wu, *et al*., Hydrogen peroxide sensor HPCA1 is an LRR receptor kinase in Arabidopsis. *Nature* **578**, 577–581 (2020).

40. C. H. Marchand, *et al*., Thioredoxin targets in Arabidopsis roots. *Proteomics* **10**, 2418–2428 (2010).

41. Y. H. Cho, S. D. Yoo, J. Sheen, Regulatory Functions of Nuclear Hexokinase1 Complex in Glucose Signaling. *Cell* **127**, 579–589 (2006).

42. S. C. Kim, L. Guo, X. Wang, Nuclear moonlighting of cytosolic glyceraldehyde-3-phosphate dehydrogenase regulates Arabidopsis response to heat stress. *Nat. Commun.* **11**, 1–15 (2020).

43. Y. Li, W. Liu, H. Zhong, H. L. Zhang, Y. Xia, Redox-sensitive bZIP68 plays a role in balancing stress tolerance with growth in Arabidopsis. *Plant J.* **100**, 768–783 (2019).

Figures legends

Figure 1. A light-independent sugar-regulated transcriptome of Arabidopsis. (A) Two week old seedlings were grown in the dark for 72 h, then transferred to 10 mM mannitol (Dark) or sucrose (Suc) in the dark, or into the light with 10 mM mannitol (Light) or 20 µM DCMU and 10 mM mannitol (DCMU). Shoot tissue was collected at 0, 0.5, 2 and 8 h for RNA-Seq. (B) Leaf glucose content in seedlings grown as in (A) (means ± SD, $N = 3$; * $P < 0.05$ from Dark; Bonferroni-corrected *t*-test). (C) Venn diagrams of differentially expressed genes at each time-point in samples collected in the dark (left) or light (right). (D) Expression trajectories of 14 clusters of co-expressed genes identified by variational Bayesian Gaussian mixture model. Pink and blue lines indicate genes identified as up/down or down/up regulated by sucrose/DCMU, respectively. The number of genes within each cluster are in parentheses. (E) Gene Ontology enrichment maps of the top 15 terms in each cluster in (D). Node colours correspond to the cluster(s) represented in (D). Node sizes are proportional to the number of genes. Selected nodes are labelled with significantly enriched, representative GO terms for each network. See Dataset 4 for the fully annotated networks.

Figure 2. Sucrose promotes superoxide production and ROS-regulated transcripts in dark-adapted seedlings. Transcript levels of representative ROS-associated genes identified as sugar-regulated from RNA-seq that are (A) from the GO class 'responsive to oxygen-containing compound' or (B) identified from a previous study (19) (means ± SD, $N = 3$). (C) Histochemical stains for hydrogen peroxide (DAB) and superoxide (NBT) in 10 d old, dark-adapted Col-0 seedlings treated with 30 mM mannitol or sucrose. (D) DAB and NBT stain intensity in seedlings grown as in (C) (means ± SD, $N = 6$; $P < 0.05$ from mannitol; Bonferroni-corrected *t*-test). (E) L-

012 luminescence in dark-adapted Col-0 treated with 30 mM mannitol or sucrose (means ± SEM, $N = 6$).

Figure 3. Modifiers of superoxide inhibit responses to sucrose. (A) Luciferase luminescence in dark-adapted *CCR2p:LUC* seedlings treated with 30 mM mannitol or sucrose in the presence of DMSO, 10 µM DPI, 2 µM MV or 200 µM 3-AT (means ± SEM, $N = 6$). (B) L-012 luminescence in dark-adapted Col-0 treated as in (A) (means ± SEM, $N = 6$). (C) Histochemical NBT stain for O_2^- and DAB stains for H_2O_2 in dark-adapted Col-0 seedlings treated with 30 mM mannitol or sucrose in the presence of 0.1% DMSO or 10 µM DPI. (D) Stain intensity in Col-0 seedlings 4 h (NBT) or 0.5 h (DAB) after treatment as in (A) ($N = 6$; * $P < 0.05$; *t*-test). (E) Inhibition of response of luciferase luminescence to 30 mM sucrose in dark-adapted *CCR2p:LUC* seedlings in the presence of 0 (0.1% DMSO), 1, 5 or 25 µM DPI. (means ± SEM, $N = 3$; * $P < 0.05$ from DMSO; Bonferroni-corrected *t*-test). (F) Transcript level of *CCR2* and *WRKY60,* relative to *UBQ10* in dark-adapted Col-0 seedlings 8 h after treatment with 30 mM mannitol, sucrose or sucrose with 10 µM DPI (means ± SD, $N = 4$; * $P < 0.05$ from mannitol; Bonferroni-corrected *t*-test. (G) Hypocotyl length and root length of 5 d old dark-grown Col-0 seedlings grown on ½ MS with or without 30 mM mannitol or sucrose, 0.1% DMSO or 1 µM DPI (means ± SD, $N = 10$; * $P < 0.05$ from ½ MS; Bonferroni-corrected *t*-test).

Figure 4. Modifiers of superoxide affect modulation of circadian rhythms by sucrose. (A) Normalised luciferase luminescence in *TOC1p:LUC* seedlings in continuous low light with 30 mM mannitol (blue) or sucrose (red) in the presence of 0.1% DMSO or 10 µM DPI, 2 µM MV or 200 µM 3-AT (means ± SD, $N = 4$). (B) Circadian period estimates of luciferase luminescence in *TOC1p:LUC* seedlings in (A) (means ± SD, $N = 4$; * $P < 0.05$ from mannitol; Bonferroni-corrected *t*-test). (C) Luciferase luminescence in *TOC1p:LUC, PRR7p:LUC* and *CCA1p:LUC* seedlings for 24 h in light/dark treated as in (A) (means ± SD, $N = 4$). (D) Phase of rhythmic O_2^-- and H_2O_2-responsive transcripts in continuous light. Values are enrichment (observed/expected) of up- and down-regulated genes in each 4-h phase window (* $P < 0.01$; χ^2).

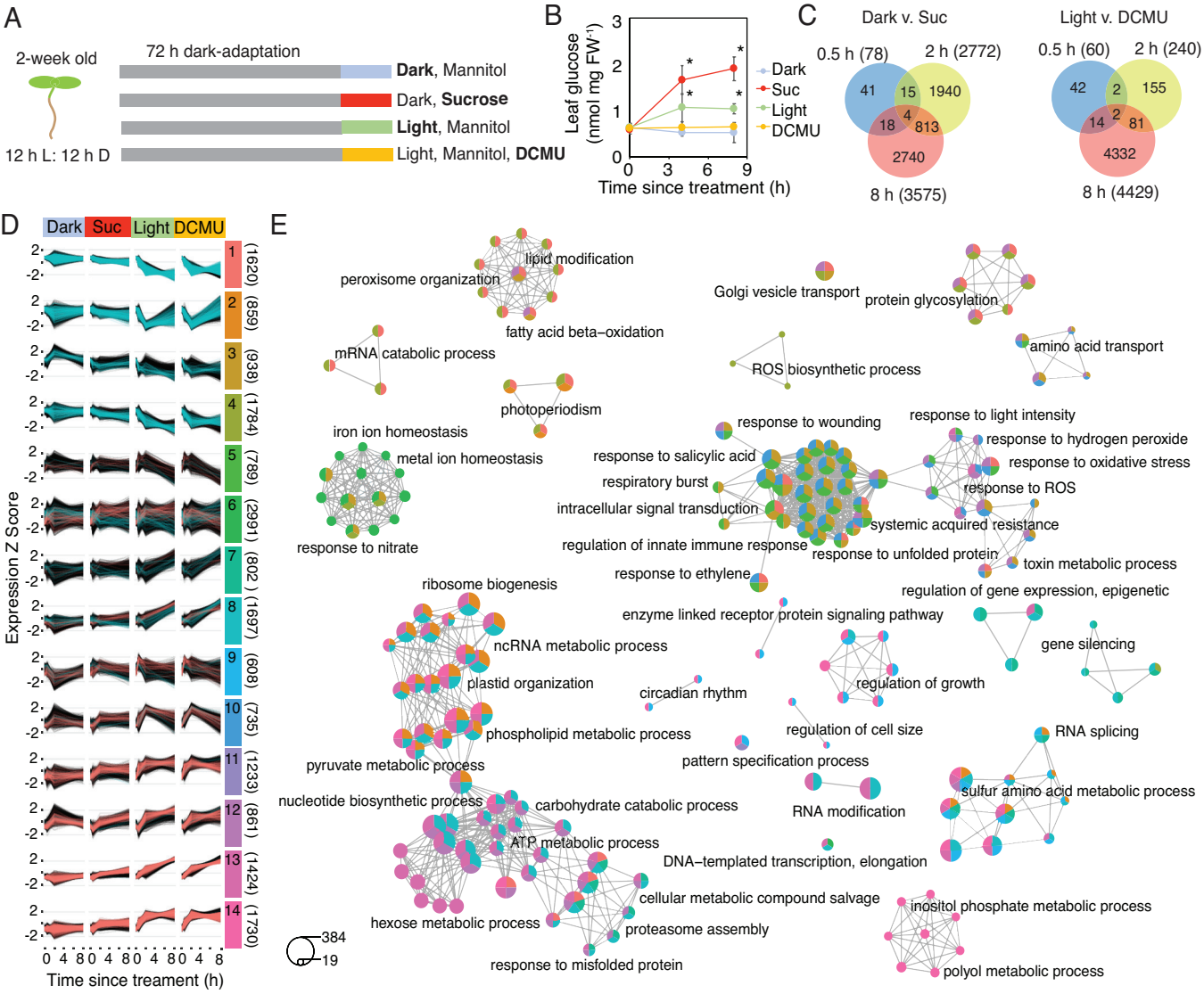
A
2-week old
72 h dark-adaptation
Dark, Mannitol
Dark, Sucrose
Light, Mannitol
Light, Mannitol, DCMU
12 h L: 12 h D
B
Leaf glucose (nmol mg FW-1)
Time since treatment (h)
Dark
Suc
Light
DCMU
C
Dark v. Suc
0.5 h (78)
2 h (2772)
8 h (3575)
41
15
1940
4
18
813
2740
Light v. DCMU
0.5 h (60)
2 h (240)
8 h (4429)
42
2
155
14
2
81
4332
D
Dark
Suc
Light
DCMU
Expression Z Score
Time since treament (h)
1 (1620)
2 (859)
3 (938)
4 (1784)
5 (789)
6 (2991)
7 (802)
8 (1697)
9 (608)
10 (735)
11 (1233)
12 (861)
13 (1424)
14 (1730)
E
lipid modification
peroxisome organization
fatty acid beta−oxidation
mRNA catabolic process
photoperiodism
iron ion homeostasis
metal ion homeostasis
response to nitrate
Golgi vesicle transport
protein glycosylation
amino acid transport
ROS biosynthetic process
response to wounding
response to light intensity
response to hydrogen peroxide
response to oxidative stress
response to ROS
response to salicylic acid
respiratory burst
intracellular signal transduction
systemic acquired resistance
regulation of innate immune response
response to unfolded protein
toxin metabolic process
response to ethylene
regulation of gene expression, epigenetic
enzyme linked receptor protein signaling pathway
gene silencing
ribosome biogenesis
ncRNA metabolic process
plastid organization
circadian rhythm
regulation of growth
phospholipid metabolic process
regulation of cell size
RNA splicing
pyruvate metabolic process
pattern specification process
nucleotide biosynthetic process
carbohydrate catabolic process
RNA modification
sulfur amino acid metabolic process
ATP metabolic process
DNA−templated transcription, elongation
cellular metabolic compound salvage
hexose metabolic process
proteasome assembly
inositol phosphate metabolic process
response to misfolded protein
polyol metabolic process
384
19

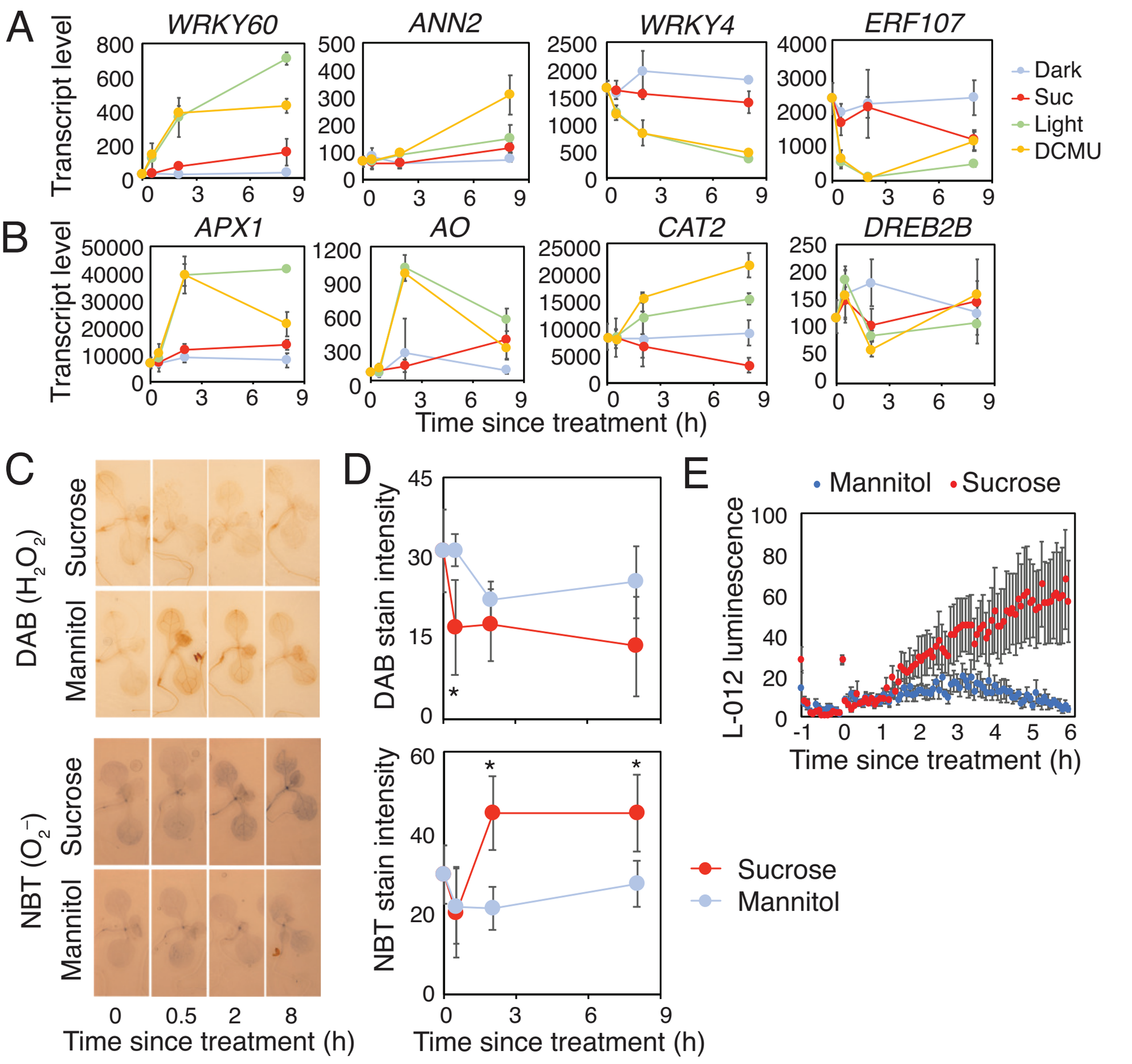
A
WRKY60
ANN2
WRKY4
ERF107
Transcript level
Dark
Suc
Light
DCMU
B
APX1
AO
CAT2
DREB2B
Transcript level
Time since treatment (h)
C
DAB (H_2O_2)
Sucrose
Mannitol
NBT (O_2^-)
Sucrose
Mannitol
0
0.5
2
8
Time since treatment (h)
D
DAB stain intensity
NBT stain intensity
Time since treatment (h)
E
Mannitol
Sucrose
L-012 luminescence
Time since treatment (h)
Sucrose
Mannitol

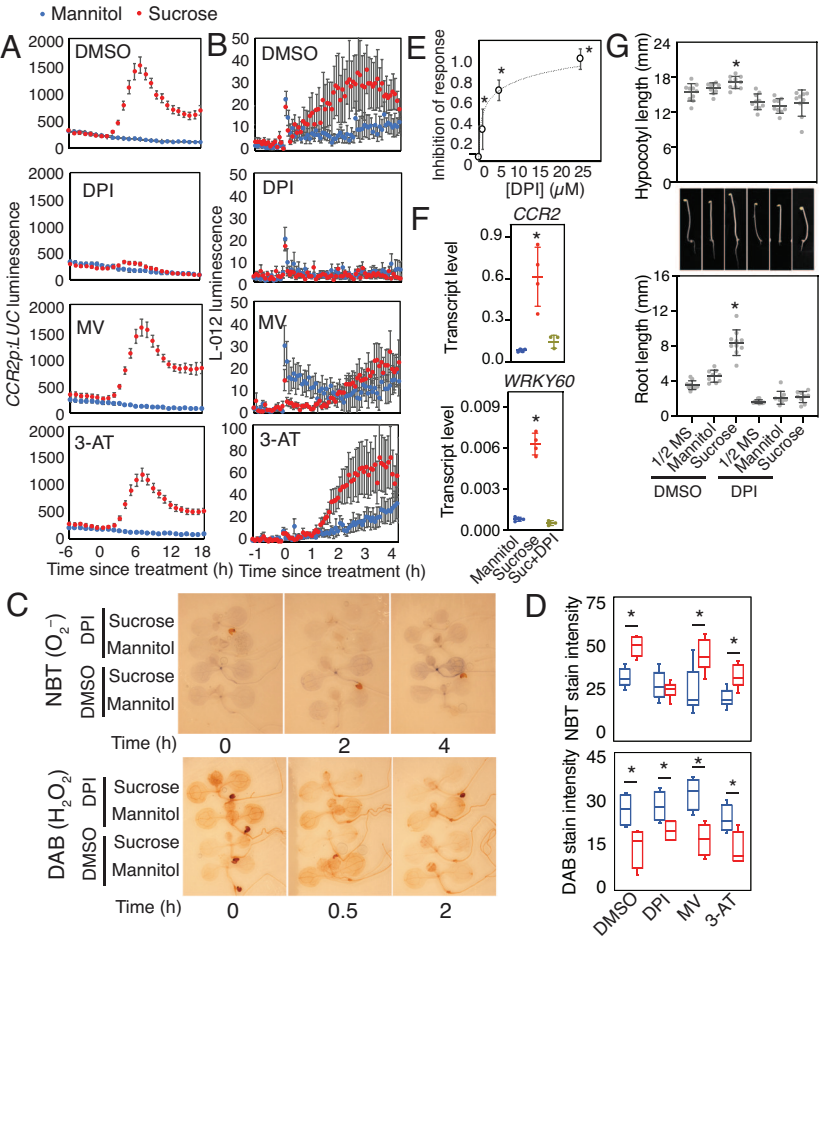
Mannitol
Sucrose
A
DMSO
DPI
MV
3-AT
CCR2p:LUC luminescence
Time since treatment (h)
B
DMSO
DPI
MV
3-AT
L-012 luminescence
Time since treatment (h)
E
Inhibition of response
[DPI] (μM)
F
CCR2
Transcript level
WRKY60
Transcript level
Mannitol
Sucrose
Suc+DPI
G
Hypocotyl length (mm)
Root length (mm)
1/2 MS
Mannitol
Sucrose
DMSO
DPI
C
NBT (O2−)
DAB (H2O2)
DPI
DMSO
Sucrose
Mannitol
Time (h)
0
2
4
0.5
D
NBT stain intensity
DAB stain intensity
DMSO
DPI
MV
3-AT

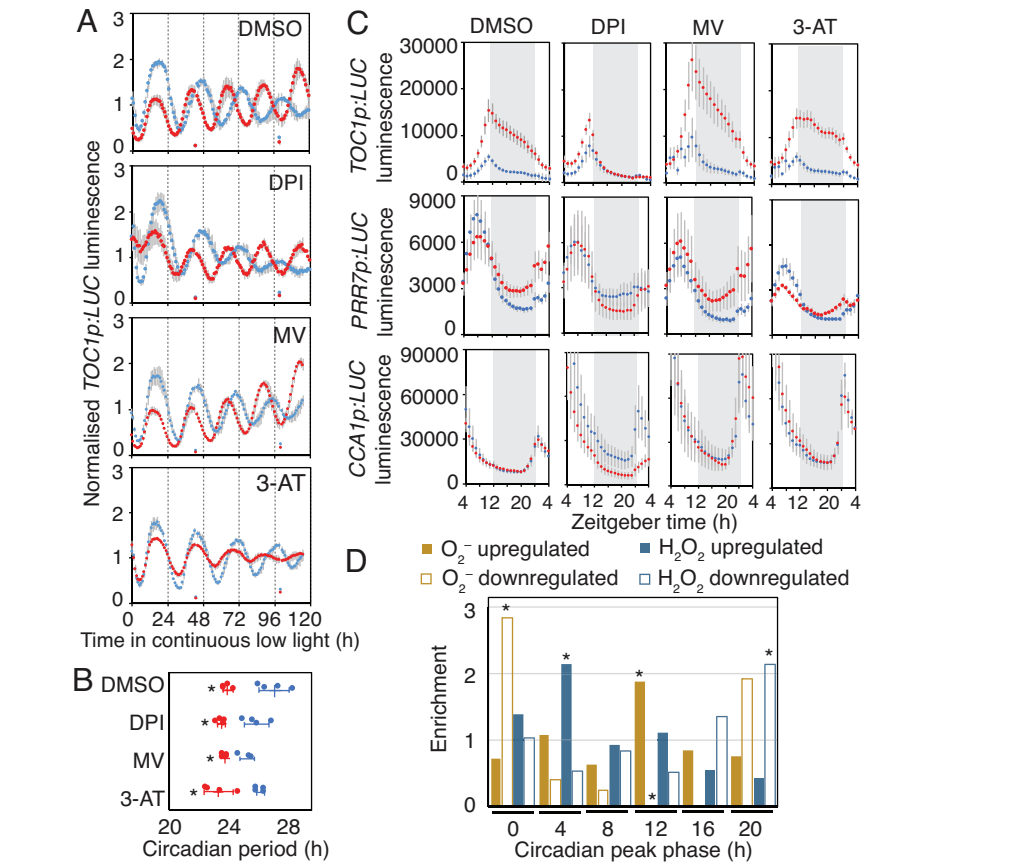
A
DMSO
DPI
MV
3-AT
Normalised TOC1p:LUC luminescence
0 24 48 72 96 120
Time in continuous low light (h)
B
DMSO
DPI
MV
3-AT
20 24 28
Circadian period (h)
C
DMSO
DPI
MV
3-AT
TOC1p:LUC luminescence
PRR7p:LUC luminescence
CCA1p:LUC luminescence
4 12 20 4
Zeitgeber time (h)
D
O2− upregulated
O2− downregulated
H2O2 upregulated
H2O2 downregulated
Enrichment
0 4 8 12 16 20
Circadian peak phase (h)

PNAS
www.pnas.org

Supplementary Information for

Superoxide is promoted by sucrose and affects amplitude of circadian rhythms in the evening

Ángela Román, Xiang Li, Dongjing Deng, John W. Davey, Sally James, Ian A Graham, Michael J Haydon

Michael J. Haydon
Email: m.haydon@unimelb.edu.au

This PDF file includes:

- Supplementary text
- Figures S1 to S10
- Legends for Datasets 1 to 6
- SI References

Other supplementary materials for this manuscript include the following:

- Datasets 1 to 6

Supplementary Information Text

Materials and Methods

Plant materials and growth conditions. Col-0 was used as wild-type *Arabidopsis thaliana*. *CCR2p:LUC, CCA1p:LUC, PRR7p:LUC* and *TOC1p:LUC* transgenic lines have been described previously (1). Mutants *rboha, rbohb, rbohc/root hair defective2-1* and *rbohd rbohf* and *WRKY11p:GUS* and *WRKY30p:GUS* transgenic lines were obtained from Arabidopsis Biological Resource Centre (ABRC). Mutant *tps1-12* (2) was backcrossed twice to Col-0.

Seeds were surface sterilised with 30% (v/v) bleach, 0.02% (v/v) Triton X-100, washed three times with sterile deionised water and sown on ½ strength Murashige & Skoog (½ MS), pH 5.7 or modified Hoagland media, pH 5.7 (3) solidified with 0.8% (w/v) agar Type M (Sigma). After 2 d in the dark at 4ºC, seedlings were grown at 20ºC in 12 h light/12 dark cycles (LD) under 100-140 µmol m^{-2} s^{-1} light. Concentrations of DPI, MV and 3-AT were based on a previous study (4)

For dark growth assays, seeds were germinated on ½ MS in LD for 48 h. Within 1 h of dawn before photomorphogenesis, germinated seeds were transferred to ½ MS with 1% (w/v) agar containing treatments, wrapped in foil and grown vertically for 3 d. Plates were photographed and root and hypocotyl lengths were quantified with ImageJ (NIH).

RNA-seq. Col-0 seeds were sown on nylon membrane on modified Hoagland's solution and grown at 45º angle. Two week old seedlings were wrapped in aluminium foil before dawn and grown in the dark for 72 h. Under dim green light, dark-adapted seedlings were transferred to Hoagland's media containing 10 mM mannitol or 10 mM sucrose and maintained in the dark or 10 mM mannitol with or without 20 µM DCMU and returned to the light. Shoots of 40 seedlings were collected at 0, 0.5, 2 and 8 h after treatments, snap-frozen in liquid nitrogen and stored at -80ºC until processing. The RNA-seq samples were taken from two independent experiments; the first produced three biological replicates for all conditions, and the second, three further replicates for the dark-grown 0, 2 and 8 h conditions. RNA was extracted with RNeasy Plant Mini Kit including on-column DNase treatment (Qiagen). RNA quantity and purity were confirmed using a Nanodrop spectrophotometer (ThermoScientific), and samples were run on an Agilent 2100 Bioanalyzer, with RNA 6000 Nano kit, to confirm RNA integrity (all samples displayed RINs of > 7). mRNA sequencing libraries were prepared from 1 µg total RNA using the NEBNext RNA Ultra Directional Library preparation kit for Illumina (New England BioLabs Inc.), in conjunction with the NEBNext Poly(A) mRNA Magnetic Isolation Module and NEBNext multiplex oligos for Illumina (dual 8 bp indexing primers set 1), according to the manufacturer's instructions. Libraries were pooled at equimolar ratios, and the pool was sent for 2 x 150 base paired end sequencing on a HiSeq 3000 at the University of Leeds Next Generation Sequencing Facility. Each sample was sequenced twice on two separate lanes, except replicate 3 of the light 2 h condition, which failed and was resequenced on one lane only, and replicate 1 of the 0 h condition in experiment 2, which also failed and was not resequenced. Raw reads have been uploaded to the European Nucleotide Archive, ENA accession PRJEB40453 [these will be made public on acceptance].

RNA-seq samples were quantified with Salmon v0.8.2 (5) using options -l ISR, --seqBias, --gcBias, --useVBOpt and --numBootstraps 30 and providing both lanes of sequencing for each sample as input. The reference was Araport11 files Araport11_genes.201606.cdna.fasta.gz and Araport11_GFF3_genes_transposons.201606.gtf.gz, downloaded from https://www.arabidopsis.org/download/index-auto.jsp?dir=%2Fdownload_files%2FGenes%2FAraport11_genome_release on 26 April 2017 (included in Dryad repository []). A map of transcript names to gene names to use with Salmon option -g was created with the following Unix one liner:

```
cut -f9 Araport11_GFF3_genes_transposons.201606.gtf | sort | uniq |
perl -ne 'print "$1\t$2\n" if /transcript_id "(.+)"; gene_id "(.+)";/'
> Araport11_GFF3_gene_transposons.201606.salmon.geneMap.tsv
```

Salmon output was converted to sleuth-compatible format with wasabi (https://github.com/COMBINE-lab/wasabi, commit f31c73e). These files will be included in a Dryad repository (https:datadryad.org) on acceptance but can be accessed during peer review here https://drive.google.com/drive/folders/18zc1PCFyZaRTnxTce3lVdhwPFZ11inCm/.

Differential expression was analysed with Sleuth v0.29.0 (6) with multiple testing correction by stageR v0.1.0, commit 59af4d7 (7), against the Araport11 gene annotation (8) imported from Ensembl Genomes release 36 (9) with biomaRt (10). Models were run with a log2 transformation function on the counts (log2(x+0.5)). A Sleuth model was built for each pairwise comparison (Dark vs Sucrose 0.5 h, Dark vs Sucrose 2 h, Dark vs Sucrose 8 h, Light vs DCMU 0.5 h, Light vs DCMU 2 h, Light vs DCMU 8 h) with differentially expressed genes detected with a Wald test for each comparison. A full model was run on all samples including control 0 h samples with differentially expressed genes detected with a likelihood ratio test. Screening p-values for stageR were taken from the full model's likelihood ratio test and confirmation p-values from the pairwise models' Wald tests. stageR results targeted a 10% overall false discovery rate using the Holm method for family-wise error rate correction. R code to run Sleuth and stageR analyses is provided in our Dryad repository (run_sleuth.R, run_stageR.R). Comparisons between gene lists were made using a Venn diagram tool http://bioinformatics.psb.ugent.be/webtools/Venn/. Gene ontology (GO) enrichment of these lists used PANTHER Classification System (11) accessed through The Arabidopsis Information Resource (TAIR).

qRT-PCR. cDNA was prepared from 0.5 µg RNA in 10 µl reactions using Tetro cDNA synthesis kit (Bioline). 0.5 ng/µl of cDNA was used in each PCR reaction with 0.2 µM primers in the SensiFAST SYBR no-ROX kit (Bioline) on a CFX96 Touch Real-time PCR detection system (Bio-Rad). PCR reaction efficiencies were determined for each primer pair using LinRegPCR (12) and transcript levels were determined for target and reference genes using (mean PCR efficiency)$^{-Ct}$. Primer sequences are listed in Dataset 5.

Transcriptome Clustering. Genes were clustered based on Sleuth scaled_reads_per_base abundance values for each sample, using scikit-learn's BayesianGaussianMixture (13) https://scikit-learn.org/stable/modules/generated/sklearn.mixture.BayesianGaussianMixture.html) with maximum 1000 iterations. Numbers of clusters from 2 to 20 were tested, with the 14 cluster output chosen for further analysis. Gene Ontology Enrichment analysis for each cluster was performed with R's clusterProfiler (14) https://bioconductor.org/packages/release/bioc/vignettes/clusterProfiler/inst/doc/clusterProfiler.html). R code for clustering is provided in the Dryad repository (cluster_analysis.R).

Histochemical stains. Seeds were sown on ½ MS and grown in LD and 11 d old seedlings were wrapped in aluminium foil at dusk. After 72 h, at subjective dusk under dim green light, seedlings were transferred into 0.5 ml liquid ½ MS containing 0.1% (v/v) DMSO or chemical treatments in 48-well plates. At the following subjective dawn in dim green light, 0.5 ml of 60 mM mannitol or sucrose was added (30 mM final sugar concentration). For H_2O_2 stains, 1 mg/ml (w/v) 3'3-diaminobenzidine tetrahydrochloride hydrate was dissolved in 50 mM Tris acetate (pH 5.0). For O_2^- stains, 2 mg/ml (w/v) nitroblue tetrazolium was dissolved in 10 mM potassium phosphate buffer (pH 7.8), 10 mM NaN_3. Seedlings were vacuum infiltrated for 1 min in freshly prepared staining solutions and incubated in the dark for 24 h. Samples were cleared by boiling for 5 min in 1:1:4 lactic acid:glycerol:ethanol then transferred to 1:4 glycerol:ethanol. GUS-stains of transgenic lines was performed overnight as previously (15). Stained seedlings were mounted under coverslips on microscope slides and imaged immediately with a SMZ800 stereomicroscope (Nikon) or a V370 Photo flatbed scanner (Epson). DAB and NBT stain intensity were quantified in whole shoots by dividing integrated density by area of individual seedlings and subtracting background signal in ImageJ (NIH).

L-012 luminescence assay. Clusters of 7 d old seedlings grown on ½ MS or 6 mm leaf discs from 4 week old plants grown in LD were transferred to 96-well luminescence plates (Greiner)

containing 250 µl liquid ½ MS before dusk (ZT12), wrapped in aluminium foil and placed in the dark for 72 h. At subjective dawn under dim green light, media was replaced with 100 µl 100 µM L-012, 20 µg/ml horseradish peroxidase containing 0.01% DMSO, 10 µM DPI, 2 µM MV, 0.2 mM 3-AT, 20 µM VAS2870, 500 µM apocynin or 500 µM allopurinol. After 1 h of chemical pre-treatment 100 µl of 60 mM sucrose or mannitol was added to each well (final sugar concentration 30 mM). Luminescence was measured in the dark at 90 s intervals in a Lumistar Omega plater reader (BMG) using a 4 mm orbital well scan.

Luciferase luminescence assays. For sugar-response assays, *CCR2p:LUC* seeds were sown on ½ MS and grown in LD. Pairs of 10 d old seedlings were transferred into 96-well luminescence plates (Greiner) containing 200 µl ½ MS with agar at dusk, wrapped in foil and grown in the dark. 1 mM D-luciferin, K-salt (Promega) was applied twice under dim green light. After 84 h in the dark (subjective dawn), 20 µl of 0.5% (v/v) DMSO, 50 µM DPI, 10 µM MV or 1 mM 3-AT was applied to seedlings under dim green light, 1 h before addition of 30 µl of 30 mM mannitol or sucrose. For the dose response curves, seedlings were transferred under dim green light to ½ MS media containing DMSO, DPI, VAS2870, apocynin or allopurinol 12 h before application of sugar at subjective dawn. Luminescence was measured in the dark at 1 h intervals in a Lumistar Omega plate reader (BMG) using a 4 mm orbital well scan.

To measure circadian rhythms, clusters of 5 seeds were sown on ½ MS and grown in LD. Clusters of 7 d old seedlings were transferred at dawn to ½ MS containing 30 mM mannitol or sucrose with 0.1% (v/v) DMSO, 10 µM DPI, 2 µM MV or 0.2 mM 3-AT. 1 mM D-luciferin, K-salt (Promega) was applied to seedlings twice prior to imaging. Luciferase was imaged in 10 min integrations following 120 s of dark at 1 hr intervals with an HRPCS5 intensified CCD camera (Photek) fitted with LB3 red (640 nm) and blue (470 nm) LED arrays providing light at 60 µmol m^{-2} s^{-1} for 1 LD followed by continuous low light at 10 µmol m^{-2} s^{-1}. Luminescence counts were extracted from ROIs using Image32 software (Photek) and circadian rhythms were analysed by Fast Fourier Transform Non-linear Least Squares using Biodare2 (16).

Sugar quantification. Seedlings were grown as for the RNA-Seq experiment or pairs of seeds were sown on ½ MS and grown in LD. Seven d old seedlings were wrapped in foil at dusk and grown in the dark. After 72 h, seedlings were transferred under dim green light into 96 well plates containing ½ MS with 0.1% DMSO or 10 µM DPI. At subjective dawn, seedlings were treated with 30 µL 30 mM mannitol or sucrose. 30 seedlings were harvested per biological replicate, frozen in liquid N and stored at -80ºC until processing. Soluble sugars were extracted in 80% (v/v) ethanol measured using a Sucrose/Glucose/Fructose calorimetric assay kit (Megazyme) scaled down for 96-well plates.

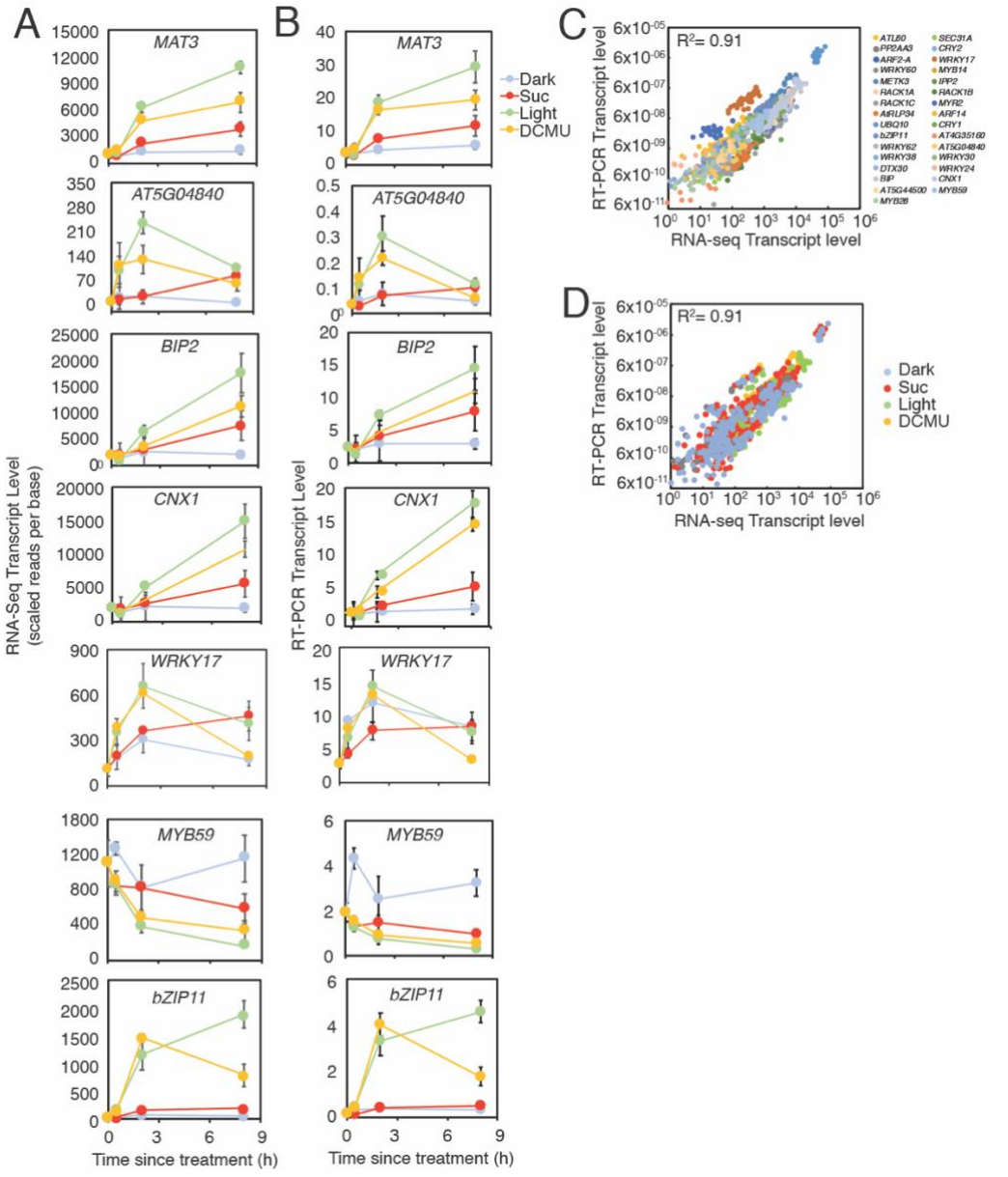

Fig. S1. Quality control of RNA-seq transcript data. (A) and (B) comparison of quantification of 8 representative marker genes determined by RNA-Seq (A) and qRT-PCR relative to geometric mean of *PP2AA3 and IPP2* (B) (means ± SD, $N = 3$). (C) and (D) comparison of quantification of 31 transcripts by qRT-PCR (PCR efficiency^{-Ct}) and RNA-seq (scaled reads per base). Plots are the same data coloured by transcript (C) or treatment (D). Values are individual biological replicates.

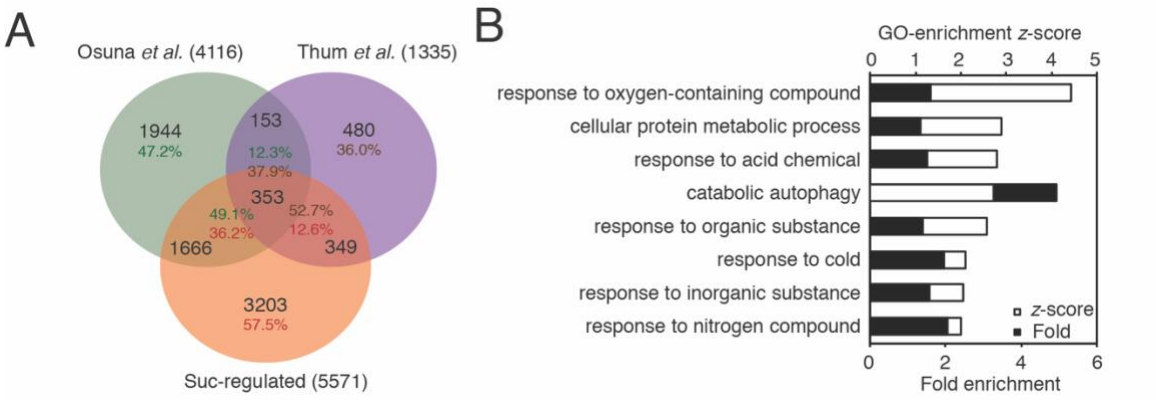

Fig. S2. Defining the light-independent sugar-regulated transcriptome in Arabidopsis shoots. (A) Comparison of genes identified as sugar-regulated in the dark in this study with two previous studies (17, 18). (B) Gene Ontology enrichment of 2772 differentially-expressed genes after 2 h treatment with mannitol or sucrose in the dark showing GO categories with a *z*-score > 2.

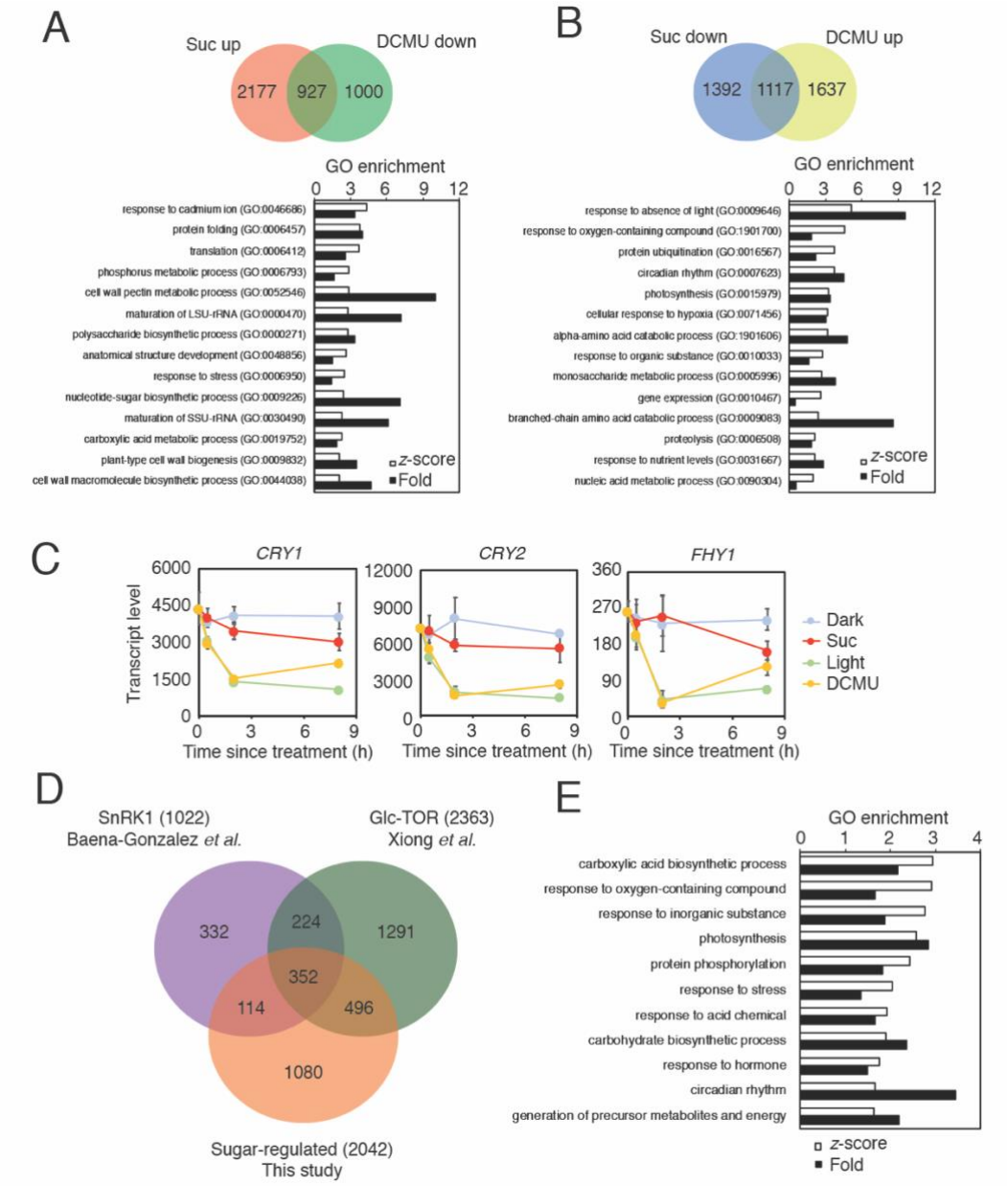

Fig. S3. Light-independent sugar-regulated genes in Arabidopsis. (A) Gene Ontology enrichment of 927 genes that are up-regulated by sucrose in the dark and down-regulated by DCMU in the light. (B) Gene Ontology enrichment of 1117 genes that are down-regulated by sucrose in the dark and up-regulated by DCMU in the light. Fold-enrichment and *z*-score are plotted on the same scale. (C) RNA-seq transcript level of light-signalling genes identified as down-regulated by sucrose and up-regulated by DCMU. (D) Comparison of 2042 genes identified as sugar-regulated in (A) and (B) to genes reported as regulated by SnRK1 (19) and TOR (20). (E) Gene Ontology enrichment of 1080 sugar-regulated genes not previously identified as SnRK1- or TOR-regulated showing GO categories with a *z*-score > 2. Fold-enrichment and *z*-score are plotted on the same scale.

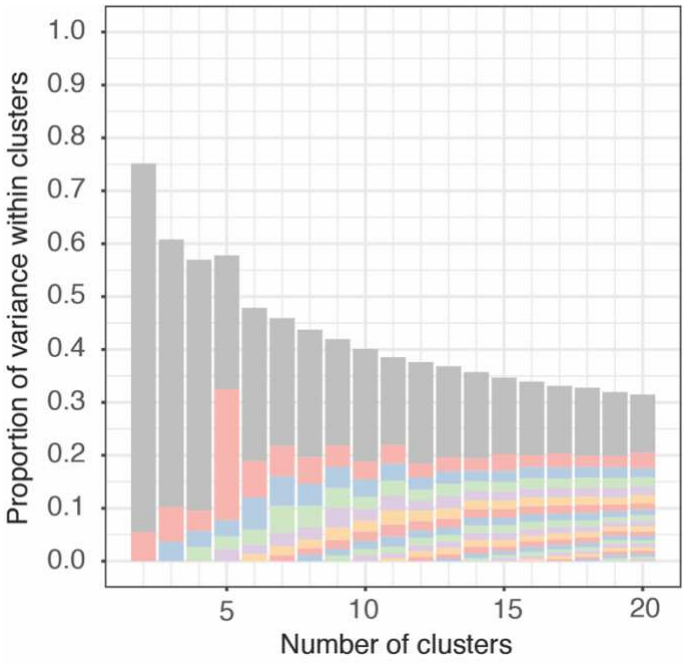

Fig. S4. Optimisation of gene clustering. Elbow plot of percentage of total variance within clusters for clustering runs with k=2 to k=20. Grey is cluster with largest variance, usually representing unclustered genes.

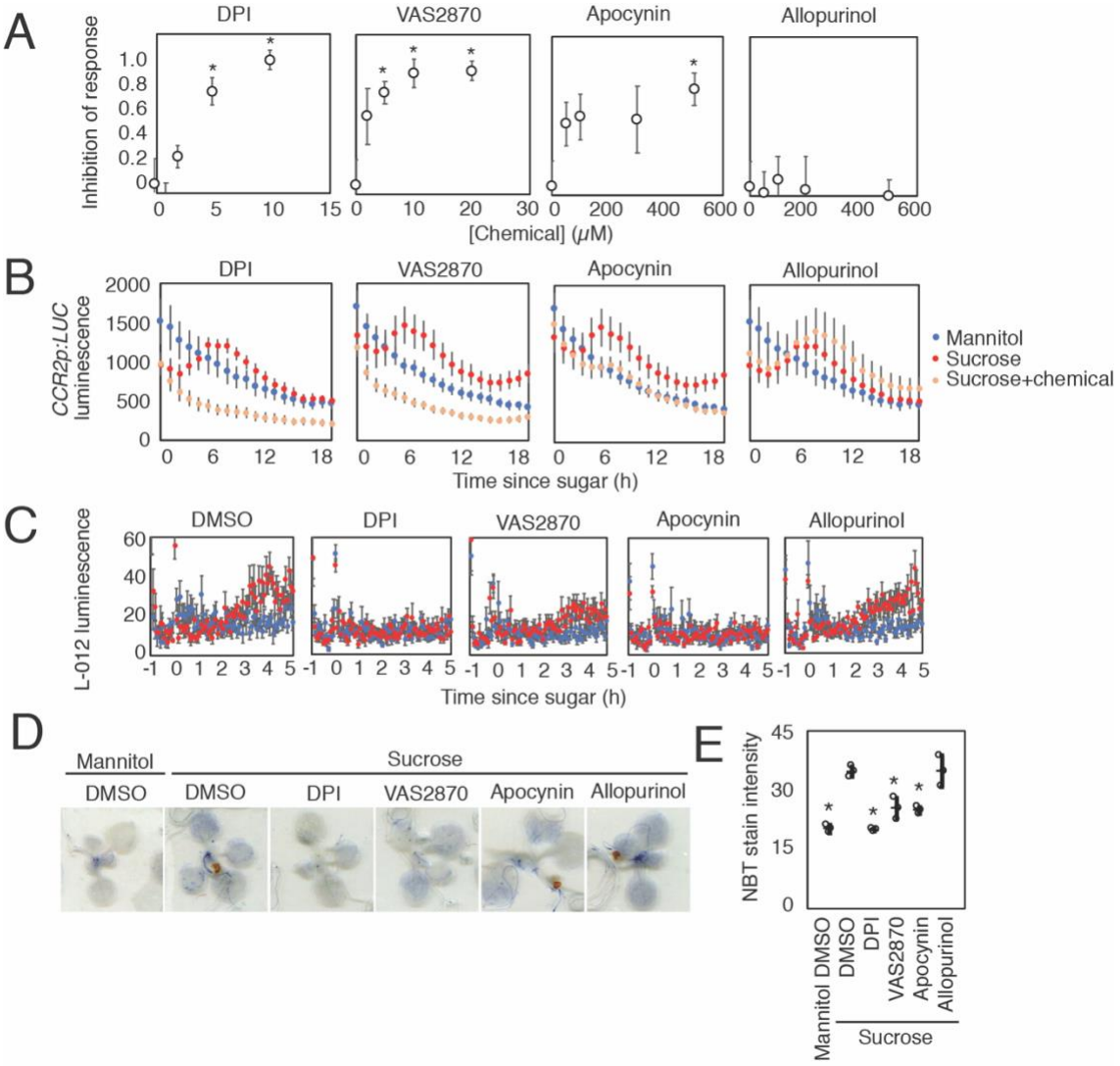

Fig S5. Effects of NADPH oxidase inhibitors. (A) Inhibition of response of luciferase luminescence to 30 mM sucrose in dark-adapted *CCR2p:LUC* seedlings by DPI, VAS2870, apocynin or allopurinol in the presence of four concentrations of each chemical inhibitor or DMSO (means ± SEM, $N = 6$; * $P < 0.05$ from DMSO; Bonferroni-corrected *t*-test). (B) Luciferase luminescence in dark-adapted *CCR2p:LUC* seedlings treated with 30 mM mannitol or sucrose in the presence of 0.1% DMSO, 10 µM DPI, 20 µM VAS2870, 500 µM apocynin or 500 µM allopurinol (means ± SEM, $N = 6$). (C) L-012 luminescence in dark-adapted Col-0 treated with 30 mM mannitol or sucrose in the presence of DMSO, 10 µM DPI, 20 µM VAS2870 or 500 µM apocynin or 500 µM allopurinol (means ± SEM, $N = 12$). (D) Representative images and (E) quantification of NBT stains in dark-adapted Col-0 seedlings 4 h after treatment with 30 mM mannitol or sucrose in presence of 0.1% DMSO, 10 µM DPI, 30 µM VAS2870, 500 µM Apocynin or 500 µM allopurinol (means ± SD, $N = 3$; * $P < 0.05$ from DMSO+Sucrose ; Bonferroni-corrected *t*-test).

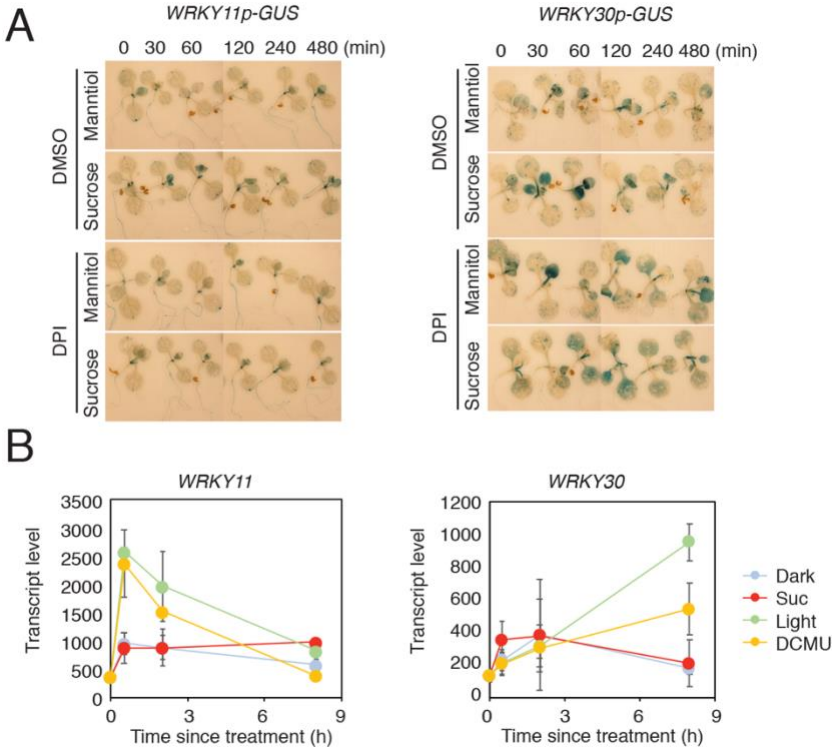

Fig. S6. Sugar and DPI affect *WRKY* promoter activity. (A) GUS stains of dark-adapted 10 d old *WRKY11p-GUS* and *WRKY30p-GUS* seedlings treated with 30 mM mannitol or sucrose, pre-treated for 30 min with DMSO or 10 µM DPI. (B) RNA-seq transcript levels of *WRKY11* and *WRKY30* (means ± SD, $N = 3$).

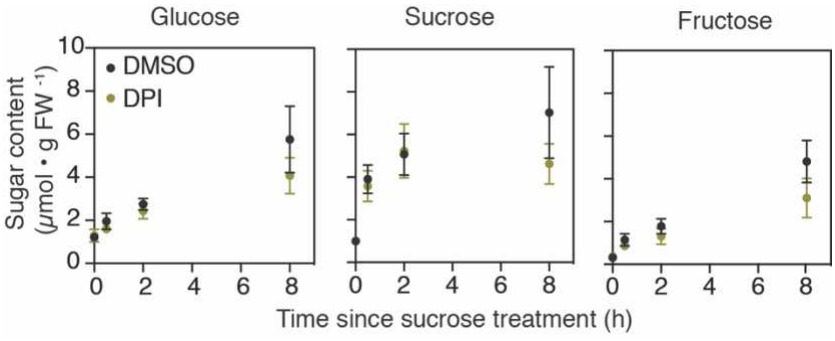

Fig. S7. Soluble sugar content in DPI-treated seedlings. Glucose, sucrose and fructose content in dark-adapted Col-0 seedlings treated with 30 mM sucrose in the presence of 0.1% DMSO or 10 µM DPI. Values are means ± SD, $N = 4$. No significant difference was identified between DMSO or DPI treated seedlings by *t*-test with Bonferroni correction, $P < 0.05$.

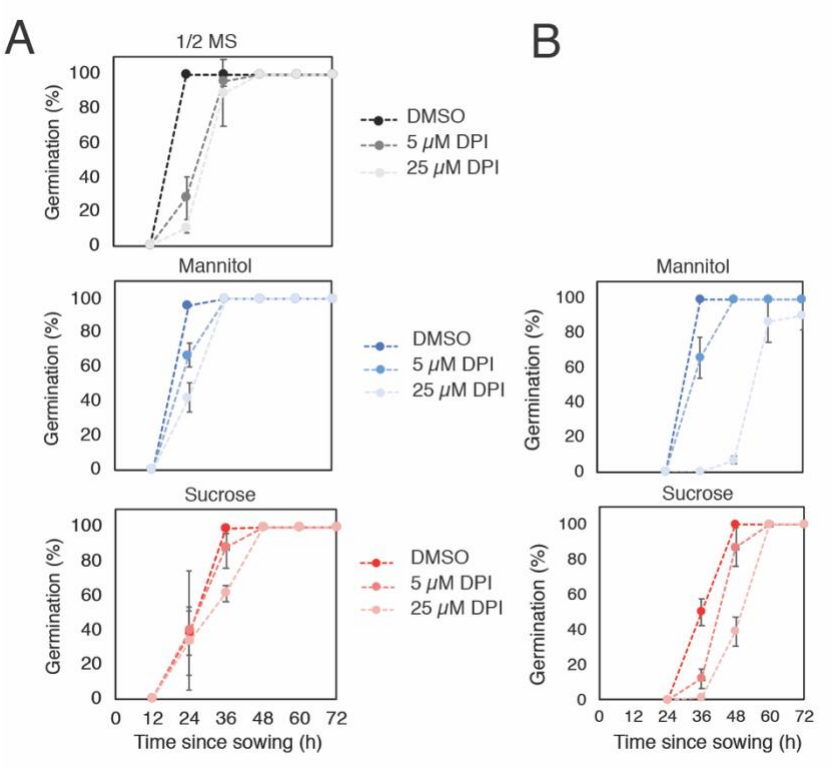

257

258 **Fig. S8.** Additive effects of DPI and sucrose on seed germination. (A) Percentage of germinated
259 (A) non-dormant Col-0 seeds following 2 d chilling at 4ºC or (B) dormant seeds without chilling
260 sown on ½ MS with or without 30 mM mannitol or sucrose and 0.1% DMSO or DPI. Values are
261 mean ± SD of four independent seed populations.
262
263

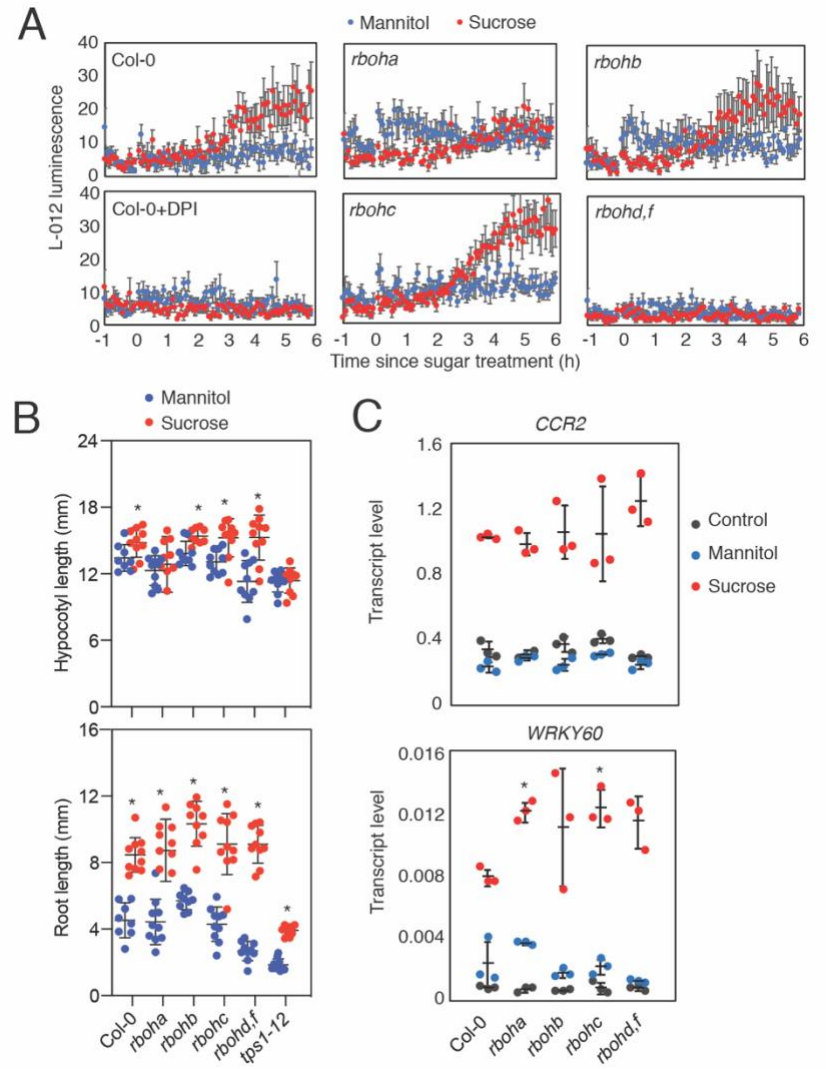

Fig. S9. NADPH oxidases contribute redundantly to sugar responses. (A) L-012 luminescence in dark-adapted Col-0 (with or without 10 µM DPI), *rboha, rbohb, rbohc* and *rbohd rbohf* seedlings after treatment with 30 mM mannitol or sucrose (means ± SEM, $N = 6$). (B) Hypocotyl length and root length of 5 d old dark-grown Col-0, *rboha, rboha, rbohb, rbohc, rbohd rbohf* and *tps1-12* seedlings grown on ½ MS with 30 mM mannitol or sucrose (means ± SD, $N = 10$; * $P < 0.05$ from mannitol, *t*-test). (C) Transcript level of *CCR2* and *WRKY60,* relative to *UBQ10* in dark-adapted Col-0 and *rboh* mutant seedlings (control) or 12 h after treatment with 30 mM mannitol or sucrose (means ± SD, $N = 3$; * $P < 0.05$ from Col-0; Bonferroni-corrected *t*-test).

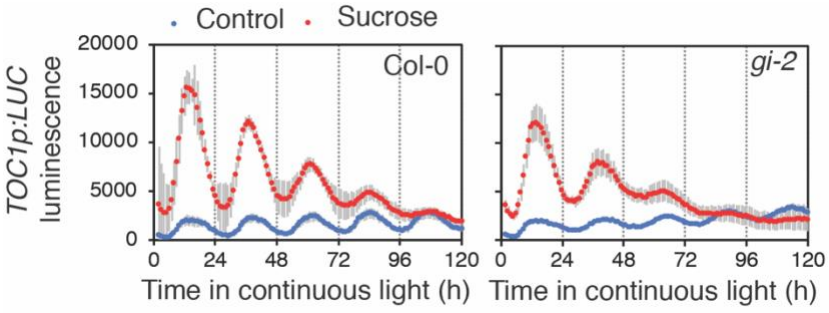

276

277

278 **Fig. S10.** Effects of ROS chemicals on circadian rhythms. Luciferase luminescence in Col-0
279 *TOC1p:LUC* and *gi-2 TOC1p:LUC* seedlings in continuous light with or without 90 mM sucrose
280 (means ± SEM, $N = 4$).
281
282

Dataset 1 (separate file). Differentially expressed genes between Dark and Suc or Light and DCMU.

Dataset 2 (separate file). Lists of sugar-activated and sugar-repressed genes.

Dataset 3 (separate file). Gene lists and GO enrichment of 14 clusters.

Dataset 4 (separate file). Complete GO enrichment map of top 15 terms from 14 gene clusters.

Dataset 5 (separate file). Gene lists and phase analysis of ROS-regulated genes.

Dataset 6 (separate file). Primer sequences.

SI References

1. M. J. Haydon, O. Mielzcarek, F. C. Robertson, K. E. Hubbard, A. a. R. Webb, Photosynthetic entrainment of the Arabidopsis circadian clock. *Nature* **502**, 689–692 (2013).
2. L. D. Gómez, A. Gilday, R. Feil, J. E. Lunn, I. A. Graham, AtTPS1-mediated trehalose 6-phosphate synthesis is essential for embryogenic and vegetative growth and responsiveness to ABA in germinating seeds and stomatal guard cells. *Plant J.* **64**, 1–13 (2010).
3. M. J. Haydon, *et al.*, Vacuolar nicotianamine has critical and distinct roles under iron deficiency and for zinc sequestration in Arabidopsis. *Plant Cell* **24**, 724–37 (2012).
4. A. G. Lai, *et al.*, CIRCADIAN CLOCK-ASSOCIATED 1 regulates ROS homeostasis and oxidative stress responses. *Proc. Natl. Acad. Sci.* **109**, 17129–17134 (2012).
5. R. Patro, G. Duggal, M. I. Love, R. A. Irizarry, C. Kingsford, Salmon provides fast and bias-aware quantification of transcript expression. *Nat. Methods* **14**, 417–419 (2017).
6. H. Pimentel, N. L. Bray, S. Puente, P. Melsted, L. Pachter, Differential analysis of RNA-seq incorporating quantification uncertainty. *Nat. Methods* **14**, 687–690 (2017).
7. K. Van den Berge, C. Soneson, M. D. Robinson, L. Clement, stageR: A general stage-wise method for controlling the gene-level false discovery rate in differential expression and differential transcript usage. *Genome Biol.* **18**, 1–14 (2017).
8. C. Y. Cheng, *et al.*, Araport11: a complete reannotation of the Arabidopsis thaliana reference genome. *Plant J.* **89**, 789–804 (2017).
9. R. J. Kinsella, *et al.*, Ensembl BioMarts: A hub for data retrieval across taxonomic space. *Database* **2011**, 1–9 (2011).
10. S. Durinck, P. T. Spellman, E. Birney, W. Huber, Mapping identifiers for the integration of genomic datasets with the R/ Bioconductor package biomaRt. *Nat. Protoc.* **4**, 1184–1191 (2009).
11. H. Mi, *et al.*, Protocol Update for large-scale genome and gene function analysis with the PANTHER classification system (v.14.0). *Nat. Protoc.* **14**, 703–721 (2019).
12. J. M. Ruijter, *et al.*, Amplification efficiency: Linking baseline and bias in the analysis of quantitative PCR data. *Nucleic Acids Res.* **37** (2009).
13. F. Pedregosa, *et al.*, Scikit-learn: Machine learning in Python. *J. Mach. Learn. Res.* **12**, 2825–2830 (2011).
14. G. Yu, L. G. Wang, Y. Han, Q. Y. He, ClusterProfiler: An R package for comparing biological themes among gene clusters. *OMICS* **16**, 284–287 (2012).
15. Á. Román, J. F. Golz, A. A. R. Webb, I. A. Graham, M. J. Haydon, Combining GAL4 GFP enhancer trap with split luciferase to measure spatiotemporal promoter activity in Arabidopsis. *Plant J.* **102**, 187–198 (2020).
16. T. Zielinski, A. M. Moore, E. Troup, K. J. Halliday, A. J. Millar, Strengths and Limitations of

Period Estimation Methods for Circadian Data. *PLoS One* **9**, e96462 (2014).
17. K. E. Thum, M. J. Shin, P. M. Palenchar, A. Kouranov, G. M. Coruzzi, Genome-wide investigation of light and carbon signaling interactions in Arabidopsis. *Genome Biol.* **5**, R10 (2004).
18. D. Osuna, *et al*., Temporal responses of transcripts , enzyme activities and metabolites after adding sucrose to carbon-deprived Arabidopsis seedlings. *Plant J.* **49**, 463–491 (2007).
19. E. Baena-González, F. Rolland, J. M. Thevelein, J. Sheen, A central integrator of transcription networks in plant stress and energy signalling. *Nature* **448**, 938–42 (2007).
20. Y. Xiong, *et al*., Glucose-TOR signalling reprograms the transcriptome and activates meristems. *Nature* **496**, 181–6 (2013).